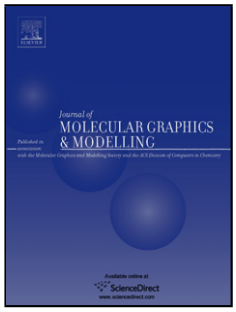

Title: Structure based virtual screening to identify selective phosphodiesterase 4B inhibitors

Author: Rahul P. Gangwal Mangesh V. Damre Nihar R. Das Gaurao V. Dhoke Anuseema Bhadauriya Rohith A. Varikoti Shyam S. Sharma Abhay T. Sangamwar

PII: S1093-3263(15)00017-0
DOI: http://dx.doi.org/doi:10.1016/j.jmgm.2015.01.007
Reference: JMG 6508

To appear in: *Journal of Molecular Graphics and Modelling*

Received date: 10-7-2014
Revised date: 30-12-2014
Accepted date: 14-1-2015

Please cite this article as: R.P. Gangwal, M.V. Damre, N.R. Das, G.V. Dhoke, A. Bhadauriya, R.A. Varikoti, S.S. Sharma, A.T. Sangamwar, Structure based virtual screening to identify selective phosphodiesterase 4B inhibitors, *Journal of Molecular Graphics and Modelling* (2015), http://dx.doi.org/10.1016/j.jmgm.2015.01.007

Graphical Abstract (for review)

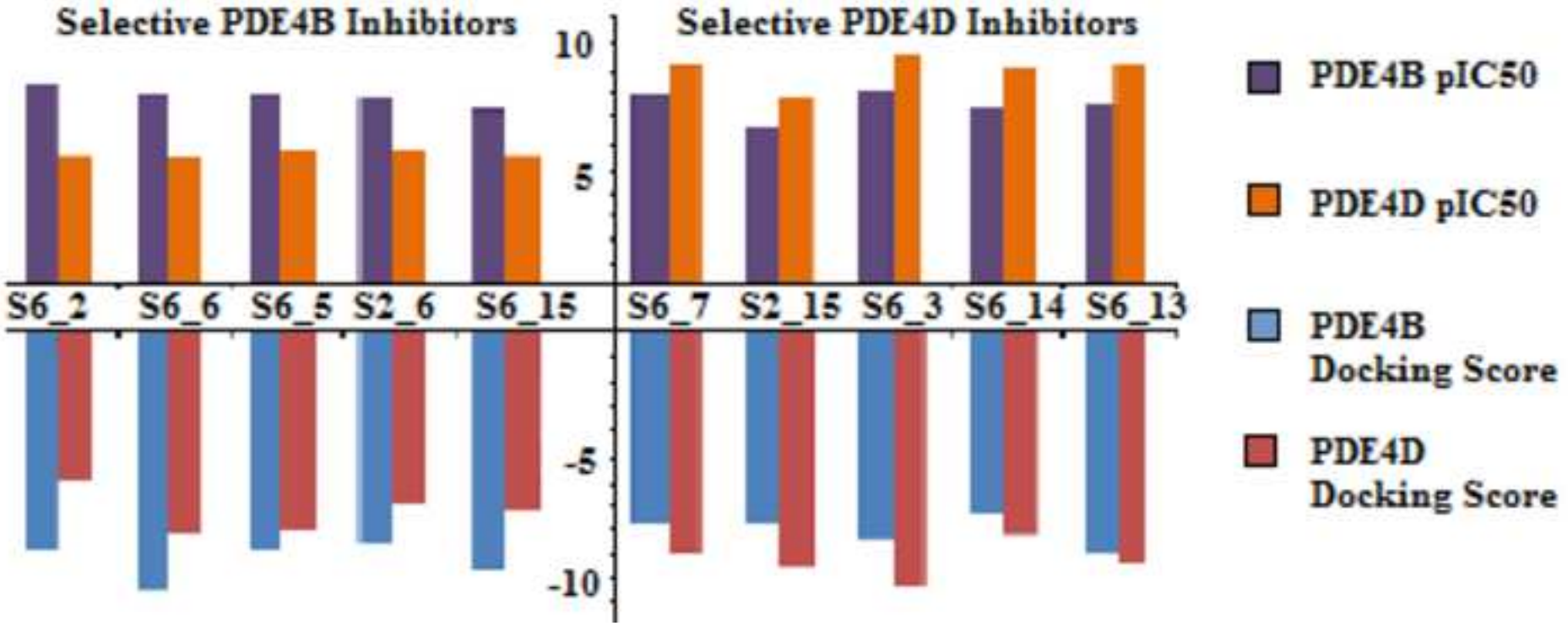

Highlights:

- Ligand based pharmacophore models were developed for PDE4B and PDE4D inhibitors.
- The developed pharmacophore model was validated by multiple approaches.
- Three different databases were screened by means of validated pharmacophore models.
- Docking analysis provided an insight into selective PDE4B inhibition.
- The results were confirmed by the *in vitro* evaluation of screened hits.

Structure based virtual screening to identify selective phosphodiesterase 4B inhibitors

Rahul P. Gangwal,[a] Mangesh V. Damre,[a] Nihar R. Das,[b] Gaurao V. Dhoke,[a] Anuseema Bhadauriya,[a] Rohith A. Varikoti,[a] Shyam S. Sharma,[b] Abhay T. Sangamwar[a,]*

[a]Department of Pharmacoinformatics, National Institute of Pharmaceutical Education and Research (NIPER), Sector-67, Mohali, Punjab-160 062, India.

[b]Department of Pharmacology and Toxicology, National Institute of Pharmaceutical Education and Research (NIPER), Sector-67, Mohali, Punjab-160 062, India.

*Corresponding author: Tel: 0172-2214682

E-mail: abhays@niper.ac.in

Abstract:

Phosphodiesterase 4 (PDE4), is a hydrolytic enzyme, is proposed as a promising target in asthma and chronic obstructive pulmonary disease. PDE4B selective inhibitors are desirable to reduce the dose limiting adverse effect associated with non-selective PDE4B inhibitors. To achieve this goal, ligand based pharmacophore modeling and molecular docking approach is employed. Pharmacophore hypotheses for PDE4B and PDE4D are generated using HypoGen algorithm. The best PDE4B pharmacophore hypothesis (Hypo1_PDE4B) consist of one hydrogen-bond acceptor and two ring aromatic features, whereas PDE4D pharmacophore hypothesis (Hypo1_PDE4D) consist of one hydrogen-bond acceptor, one hydrophobic aliphatic, and two ring aromatic features. The validated pharmacophore hypotheses are used in virtual screening to identify selective PDE4B inhibitors. The hits were screened for their estimated activity, FitValue, and quantitative estimation of drug likeness. After molecular docking analysis, ten hits were purchased for *in vitro* analysis. Out of these, six hits have shown potent and selective inhibitory activity against PDE4B with IC_{50} values ranging from 2 to 378 nM.

Keywords: COPD; Molecular docking; Phosphodiesterase; Pharmacophore; Virtual screening.

Introduction

Chronic obstructive pulmonary disease (COPD) is one of the most predominant diseases globally. COPD is considered as the 5th leading cause of death, affecting about 600 million people of average age 45 and above across the globe [1]. COPD is projected as the 3rd major cause of death by 2020 [2]. This disease is named as a multi-component because it encompasses several inflammatory pathologies of body organs like parenchymal inflammation, structural changes, airway obstruction, systemic effects, and inflammation of conducting airway of the respiratory system [3]. This leads to the progressive, irreversible damage and decrease in lung function, persistent airflow limitation due to airway collapse, edema, and fibrosis. Increase in inflammation mediators in peripheral blood, weight loss, skeletal muscle apoptosis, and nutritional abnormalities are also associated with COPD. The chronic progressive symptoms of COPD include productive cough, breathlessness and exacerbations, adversely affecting the health status of the patient [4]. Similar to COPD, there is another well-known inflammatory disease called asthma, in which cytotoxic mediators, CD+ T-lymphocyte and inflammatory cells cause an inflammatory response resulting in airflow obstruction and airway hyper-responsiveness [5]. Asthma is also characterized by blockade due to airway smooth muscle contraction (ASM). Cyclic nucleotide adenosine 3',5'-cyclic monophosphate (cAMP) is an important regulatory secondary messenger, which mediates ASM cell relaxation. Secondary messengers like cAMP and cGMP (guanosine 3',5'-cyclic monophosphate) are hydrolyzed by Phosphodiesterases (PDEs) and therefore play an essential role in the maintenance of their cellular level.

Phosphodiesterase enzymes are divided into eleven groups (PDE1–PDE11) based on the primary structure, tissue distribution and hydrolyzing property. Each family of the enzyme is further divided into different isoforms. Among the entire PDE enzyme group, the PDE4 family is predominantly associated with the COPD and asthma. The further division of this family include subtypes from Phosphodiesterase 4A to Phosphodiesterase 4D (PDE4D) [6]. PDE4 enzyme is one of the elements that controls the level of cAMP in various regions of the body, which acts as a secondary messenger and plays a key role in the regulation of most cellular functions. The whole family is known as low K_m, cAMP-selective PDE, and the rolipram-sensitive PDE. Activation of cAMP signaling in inflammatory cells has negative modulatory effects on several steps required for an immune and inflammatory response, including T cell activation and proliferation, and cytokine release, particularly the tumor necrosis factor-α (TNF-α) [7], and recruitment of leukocytes [8]. Considering these facts, pharmacological intervention of cAMP level becomes a promising approach for the treatment of chronic inflammatory conditions like asthma, COPD, and other inflammatory bowel diseases [9].

The principle therapeutic role of the PDE4 protein family was recognized through the action of first-generation PDE4 inhibitor, rolipram. The PDE4 inhibitors, such as RO-20-1724 (mesopram) and zardaverine were discontinued from the clinical trials because of the side effects like nausea, vomiting, dyspepsia, and headache [10]. As PDE4 inhibitors are non-selective towards other PDEs expressed in body cells, researchers aims to design selective PDE4 inhibitors [11, 12]. Amongst the isoforms of PDE4 family, selective inhibition of PDE4B considerably suppresses the LPS-induced TNF-α production in circulating monocytes and peritoneal macrophages [7, 8] and retain numerous beneficial anti-inflammatory effects without the dose limiting side-effects [13].

The aim of present study is to identify the basic structural requirements for selective PDE4B inhibition through ligand-based pharmacophore modeling and molecular docking approach. Two individual pharmacophore models were developed using known PDE4B and PDE4D inhibitors. These pharmacophore hypotheses were further validated and used as a 3D query for screening three different databases. A molecular docking study was carried out using Glide5.5 to reduce the total number of false positive hits. Finally, we reported six hits with diverse scaffolds as possible candidates for designing of potent and selective PDE4B inhibitors. **Fig. S1** summarizes the detailed workflow followed during this study.

Materials and methods

Data sets

The dataset of 71 inhibitors for PDE4B and 72 inhibitors for PDE4D was selected from the literature, based on the biological assay method, and subsequently used for generation of pharmacophore models [14-18]. The inhibitory activities (IC_{50} value) of PDE4B and PDE4D inhibitors were spanned across a wide range of 0.5 to 61000 nM and from 0.2 to 11000 nM, respectively.

The dataset was divided into a training and test set according to their structural diversity and activity. The selection of suitable training set is an important step in the generation of pharmacophore models, which helps in determining the quality of generated models. HypoGen pharmacophore hypotheses were generated using a set of 23 PDE4B inhibitors and set of 24 PDE4D inhibitors (**Fig. S2 and Fig. S3**). The remaining 48 compounds from the original data set were used as a test set for validation of generated pharmacophore hypotheses. Further, for evaluation purposes, the activity values were categorized on the scale of: highly active (+++, $IC_{50} < 250$ nM); moderately active (++, 250 nM $\leq IC_{50} <$ 2500 nM), and least active (+, $IC_{50} \geq 2500$ nM). The BEST method was used for generation of numerous conformation for all the inhibitors, which provides a

complete and improved coverage of the conformational space by performing a rigorous energy minimization and optimizing the conformations in both torsional and Cartesian space using the poling algorithm [19]. During this process, maximum number of conformers was set to 255 with 4.0 kcal/mol as energy cutoff, and all other parameters were set to default [20]. Pharmacophore models were then generated using the HypoGen algorithm implemented in Accelrys Discovery Studio2.5 (DS2.5) [21].

Pharmacophore modeling

The 3D QSAR Pharmacophore Generation module in the DS2.5 software package running on an IBM graphic workstation was used to generate the top ten pharmacophore hypotheses with significant statistical parameters. HypoGen module helps to identify the features that are common with the active compounds, but excludes common features for the inactive compounds within conformationally allowable regions of space. The process of a pharmacophore hypothesis is divided into three steps; constructive step, a subtractive step and an optimization step. In the constructive step, features that are common among the active compounds were identified involving simple calculation based on the activity and uncertainty value. The features common between the least active compounds were then removed in the subtractive step. The hypotheses are then optimized using simulated annealing to refine the model parameters. Considering the chemical nature of both PDE4B and PDE4D inhibitors, five features, namely hydrogen-bond acceptor (HBA), hydrogen-bond donor (HBD), hydrophobic aliphatic (HYA), hydrophobic aromatic (HYAr), and ring aromatic (R) were selected to generate the pharmacophore hypotheses. The minimum and maximum number of features to be included during pharmacophore generation was set to 0 and 5, respectively. The uncertainty value was set to the default 3, which corresponds to the biological activity of a particular inhibitor, which is assumed to be located somewhere in the range three times higher to three times lower of the true value of that inhibitor. The quality of the generated HypoGen pharmacophore hypothesis can be best described in terms of several statistical parameters, such as fixed cost, null cost and total cost. The best model among the ten generated pharmacophore hypotheses was selected based on high correlation coefficient (r), lowest total cost, highest cost difference, and a low root mean squared deviation (RMSD) values [22].

The best pharmacophore hypotheses were validated to check whether they are capable of discriminating between the active and the least active compounds, and predicting their activities accurately. For the validation of the generated pharmacophore hypothesis, three different methods (test set prediction, Fischer randomization test and decoy test) were employed. Primarily, in the cost analysis, numerous theoretical cost values (represented in bit units) were examined, namely fixed cost, null cost and the total cost. In addition to this

three other cost values such as weight cost, configuration cost, and error cost also plays a vital role in determining the quality of the generated hypotheses. In test set validation, the data set of inhibitors, as the representative of the learning series with a wide range of inhibitory activity was used to validate the best HypoGen pharmacophore hypothesis. Further, to analyze the quality of the generated hypotheses, a Fischer randomization (Cat-Scramble) test was employed to check the strong correlation between chemical structures and biological activity in the training set. To achieve a 95% confidence level, 19 random pharmacophore hypotheses were generated during the Cat-Scramble run by shuffling the activity value of the compounds in the training set [23].

Lastly, for the validation of Hypo1_PDE4B and Hypo1_PDE4D, individual decoy sets were generated using DecoyFinder1.1 [24]. Decoys were selected if they are having similarity to that of the active ligands in respect to physicochemical descriptors (molecular weight, number of rotational bonds, hydrogen bond donor count, hydrogen bond acceptor count and the octanol–water partition coefficient) and deprived of the chemical descriptors to any of the active ligands. Decoy sets were comprised of 14 PDE4B and 11 PDE4D active inhibitors to calculate various statistical parameters such as accuracy, precision, sensitivity, specificity, goodness of hit (GH) score, and enrichment factor (E value). Out of these, GH and E values are the two major parameters, which plays a significant role in identifying capability of the generated pharmacophore hypothesis.

Pharmacophore based virtual screening

Pharmacophore-based virtual screening of known chemical databases is a fast and precise method, which serves the purpose of identifying potential leads suitable for further development [25]. It has an advantage over any *de novo* design method because retrieved hits can be easily obtained for biological testing. For database screening, Fast/Flexible and Best/Flexible are the two options available in DS2.5. In our study, we have performed virtual screening using the Best/Flexible search option. Three commercially available databases, filtered by Lipinski's rule of five, were selected. The validated pharmacophore hypotheses were used as 3D query with the Best/Flexible search option for performing virtual screening of these databases. Initially, validated pharmacophore hypothesis Hypo1_PDE4B was used to screen the databases. The screened compounds having estimated IC_{50} less than 20 nM were selected and subsequently subjected to the screen by the best pharmacophore hypothesis (Hypo1_PDE4D) of PDE4D inhibitors. In both cases, the Maximum Omitted Features option was set to '-1' to screen the databases. The hit compounds, which have shown the Hypo1_PDE4B estimated FitValue less than 4 were submitted further for the evaluation of drug-likeness properties using quantitative estimation of drug likeness (QED) property. DS2.5 was used to calculate

physicochemical properties essential for QED calculation. The properties calculated were MW, ALOGP, number of HBDs, number of HBAs, molecular PSA, number of ROTBs, and the number of AROMs. Finally, a substructure search was performed against each compound using a curated reference set of 94 functional moieties that are potentially mutagenic, reactive or have unfavorable pharmacokinetic properties. The number of matches for each compound was captured (ALERTS) [26]. The unweighted and weighted QED values were calculated based on the above mentioned molecular properties by using the following formulae:

$$QED = \exp\left(\frac{1}{n}\sum_{i=1}^{n}\ln d_i\right) \quad (1)$$

$$QED_w = \exp\left(\frac{\sum_{i=1}^{n} w_i \ln d_i}{\sum_{i=1}^{n} w_i}\right) \quad (2)$$

Where *d* is the derived desirability function; w is the weight applied to each function and n is the number of molecular properties [27, 28]. Those hits passing the QED test were subjected to molecular docking using Glide5.5.

Molecular docking

To explore the intermolecular interactions between ligands and the target protein, molecular docking was performed, which further helps in the calculation of binding affinities. To achieve this goal, an automated docking program Glide5.5 [29] was used. Three-dimensional information of target protein was taken from the protein data bank (PDB ID: 1RO6 and 1TBB) [30, 31]. The Protein Preparation Wizard and LigPrep modules were used for the generation of input files necessary to carry out molecular docking. During ligand preparation, ionization states were generated using Epik module. During protein preparation, hydrogen atoms were added to the target protein and the protonation states for histidine residues were optimized. The protein structure was minimized with constraint on the heavy atoms to reach the converged root mean square deviation (RMSD) of 0.30 Å. [32]. A Receptor Grid generation tool was used to generate a grid of 10Å around the active site of prepared PDE4B and PDE4D. To validate the docking protocol, co-crystallized ligand was docked into the active site cavity of PDE4B and PDE4D. OPLS_2005 force field was used for energy minimization of designed ligands. Standard precision mode and other default settings for scaling the van der Waals radii were selected: a scaling factor of 0.8 and a partial charge cutoff of 0.25 with no constraints were defined for docking of PDE4

inhibitors and screened hit compounds. Final hits were selected based on the binding mode and molecular interactions observed in the active site.

PDE4B2 and PDE4D2 activity assay

PDE4 activity was determined for subtypes B2 and D2 using respective assay kits (Catalogue no: 60343 and 60345, respectively) from BPS Biosciences, San Diego, CA. Apart from using rolipram as standard, we screened ten compounds for their inhibitory activities. The assay kits were designed for identification of inhibitors of the respective subtype of the enzyme using fluorescence polarization. The process was based on binding of a fluorescent nucleotide monophosphate generated by subtypes B2 or D2 to the binding agents followed by its detection. Manufacturer's instruction was followed during the assay. Briefly, 25 µl of FAM-Cyclic-3´,5´-AMP (200 nM) with or without test compounds (stock solutions were prepared by dissolving in DMSO, 0.01 nM-1000 nM; 5 µl) was incubated with PDE4B2 (7.5 pg/µl; 20 µl) or PDE4D2 (2.5 pg/µl, 20 µl) for one hour. It was followed by the addition of a binding agent (100µl) to the reaction mixture in each microwell, incubated for one hour at room temperature with gentle shaking. The fluorescent polarization was measured in the Microtiter plate (Black, low binding NUNC Microtiter plate, catalogue no: VWR 62408-936) using a fluorescence reader (SpectraMax M2 & M2e Multi-Mode Microplate Reader) set for excitation at wavelengths ranging from 475-495 nm and detection of emitted light ranging from 518-538 nm. A blank value was subtracted from all other values. Plots for % activity Vs log concentration were drawn, and IC_{50} was determined using nonlinear regression curve fit method using Graph Pad Prism v5.01 (Graph Pad Software Inc.).

Results and discussion

Pharmacophore modeling

In ligand-based pharmacophore modeling studies, top 10 pharmacophore hypotheses were generated for both PDE4B and PDE4D using diverse training set compounds. The results obtained during pharmacophore hypothesis generation for PDE4B and PDE4D were summarized in **Table 1** and **Table 2,** respectively. The best pharmacophore hypothesis (Hypo1_PDE4B and Hypo1_PDE4D) for each biological target was characterized by the good correlation coefficient, lowest root mean square error, and the highest cost difference. Hypo1_PDE4B consists of spatial arrangement of three chemical features, namely, the presence of one HBA, and two R features along with five excluded volumes (**Fig. 1a**). The Hypo1_PDE4D consists of one HBA, one HYA, two R features and four excluded volumes (**Fig. 1b**). **Table S1** and **Table S2** summarize the Hypo1_PDE4B and Hypo1_PDE4D estimated activity along with their corresponding error values of PDE4B and PDE4D training

set molecules. Among twenty three PDE4B training set compounds, all highly actives (+++) and the least active compounds (+) were predicted accurately, and one moderately active (++) compound was underestimated as least active (+); while in case of PDE4D, out of twenty four training set compounds, all highly actives (+++), moderately actives (++) compounds were predicted accurately, and two least active compounds (+) were overestimated as moderately active (++). Moreover, the majority of highly active compounds of the training set were mapped to all pharmacophore features of Hypo1_PDE4B and Hypo1_PDE4D and in case of moderately active and the least active compounds, one or two features were missing. **Fig. 2a** and **Fig. 2b** shows the most active compounds from PDE4B and PDE4D inhibitors, which were mapped accurately over all the features of Hypo1_PDE4B and Hypo1_PDE4D, respectively. In case of the least active compound from PDE4B, one HBA and one R feature were missing, while in case of PDE4D, one R feature was missing, and other features were mapped partially (**Fig. 2c and Fig. 2d).** FitValue is a measure of overlap between the features in the pharmacophore and chemical features in the molecule, which assist in understanding the chemical meaning of the pharmacophore hypothesis. The most active compound in the training set of PDE4B and PDE4D inhibitors has shown the fitness score of 4.79 and 8.84, whereas the least active compound has shown the fitness score of 0.68 and 4.54 when mapped to Hypo1_PDE4B and Hypo1_PDE4D hypothesis, respectively.

Pharmacophore model validation

Validation is one of the important steps in pharmacophore generation. Several methods and parameters are available to confirm the quality of a generated pharmacophore model like cost analysis, test set prediction, Fischer's randomization method, goodness of fit, and enrichment factor. During pharmacophore generation, various cost values were calculated. The difference of 40–60 bits between the total cost and the null cost hypotheses signifies the 75–90% chance of representing a true correlation in the data. The total cost value for hypotheses Hypo1_PDE4B and Hypo1_PDE4D was 98.265 and 101.136, while null cost value was 146.531 and 185.932, respectively. The cost difference between the null cost and total cost value for the Hypo1_PDE4B was 48.266, whereas for Hypo1_PDE4D was 84.796, which characterizes that both the pharmacophore hypotheses can significantly correlate the data. Both pharmacophore hypotheses Hypo1_PDE4B and Hypo1_PDE4D have shown the highest correlation coefficient value of 0.956 and 0.988, respectively. In addition, RMSD values were 0.720Å and 0.466Å, respectively. The configuration cost value for Hypo1_PDE4B and Hypo1_PDE4D was 12.909 and 15.088, respectively. Amongst the generated ten pharmacophore hypotheses, Hypo1_PDE4B and Hypo1_PDE4D have shown better statistical values, including higher correlation, greater cost difference, lower RMSD and configuration cost values. Based on the validation results, these hypotheses were considered as the

best pharmacophore hypotheses for subsequent validation. The second step includes the activity prediction of test set compounds. Both pharmacophore hypotheses were used to estimate the activity of the test set compounds. Most of the compounds in the PDE4B and PDE4D test sets were predicted correctly with respect to their experimental biological activity. A coefficient of determination (r^2) of 0.713 and 0.723 for PDE4B and PDE4D test set, respectively, shows that there is good correlation between the experimental and predicted activities (**Fig. 3**). In PDE4B test set validation, it was found that 20 of 27 highly active, 12 of 17 moderately active, and 3 of 4 least active compounds were predicted correctly. Seven highly active compounds were underestimated as moderately active, while five moderately active compounds were underestimated as least active and one least active compound was overestimated as moderately active. Likewise, in PDE4D test set validation, 22 of 24 highly active, 7 of 14 moderately active and 3 of 10 the least active compounds were predicted correctly. Two highly active compounds were underestimated as moderately active and three moderately active compounds were overestimated as actives and four were underestimated as the least active compounds. Also, seven least active compounds were overestimated as moderately active. Fischer randomization test (Cat-Scramble) was employed as a second validation process to attain the 95% confidence level. Randomly, 19 pharmacophore hypotheses were generated for both PDE4B and PDE4D training set, which were compared with the original pharmacophore hypotheses Hypo1_PDE4B and Hypo1_PDE4D, respectively. **Fig. 4a** and **Fig. 4b** show that none of the randomly generated pharmacophore hypotheses have scored better statistical results than Hypo1_PDE4B and Hypo1_PDE4D, respectively. The results obtained during Cat-Scramble run indicate that hypotheses Hypo1_PDE4B and Hypo1_PDE4D have not been generated by any chance correlation.

Finally, DecoyFinder1.1 was employed to generate small databases (D) containing 518 and 407 compounds, which includes 14 and 11 actives; 834 and 731 decoys for PDE4B and PDE4D, respectively. These databases were used to validate the best hypotheses (Hypo1_PDE4B and Hypo1_PDE4D) for distinguishing the actives from decoys or not. Both the hypotheses, Hypo1_PDE4B and Hypo1_PDE4D were used as a 3D structural query to perform screening of several databases. The accuracy, precision, sensitivity, and specificity of the best pharmacophore models were calculated. Furthermore, for the analysis of results, E value and GH score were calculated using the following formulae:

$$E = \frac{(TP \times D)}{(Ht \times A)} \tag{3}$$

$$GH = (TP/4HtA)(3A + Ht) \times (1 - ((Ht - TP)/(D - A))) \tag{4}$$

Where D, A, Ht and TP represent the total number of compounds of the database, total number of actives, total number of hits and total number of true actives in the hits, respectively [20]. Hypo1_PDE4B and Hypo1_PDE4D have shown an E value of 21.14 and 24.66, respectively. The calculated GH score for both hypotheses was greater than 0.6, which specifies that the quality of developed pharmacophore was significant (**Table 3**). From the overall validation results, we assure that hypotheses (Hypo1_PDE4B and Hypo1_PDE4D) can differentiate between the actives and decoys.

Pharmacophore model based virtual screening

Virtual screening (VS) approach is proven as an important tool in medicinal chemistry to speed up drug development process. The sequential order followed during the virtual screening process to identify selective PDE4B inhibitors is shown in **Fig. S4**. Initially, the validated pharmacophore model (Hypo1) of PDE4B inhibitors was used as a query to search the NCI, Specs, and ChemDiv databases, which were pre-filtered using the Lipinski's rule of five. A set of 748822 hits, mapping to the pharmacophore model Hypo1_PDE4B was retrieved, which comprised of some compounds structurally similar to that of the existing PDE4B inhibitors, and some novel scaffolds were also emerged. The 14620 hit compounds showing Hypo1_PDE4B estimated IC_{50} less than 20 nM were selected and subsequently subjected to screen using the validated pharmacophore model Hypo1_PDE4D. The 326 hit compounds were chosen that showed Hypo1_PDE4D estimated FitValue less than 4 and submitted for their QED value calculation.

QED values contribute in screening chemical structures by their merit relative to the target functions. QED value gives a better view of drug likeness in contrast to the rule-based approaches. Principally, the QED value depends upon the distribution of molecular properties, opposing the rule-based metrics. In some cases, it also identifies a generally unfavorable property that may be tolerated when the other parameters are close to the ideal. The unweighted_QED and weighted_QED values were calculated for screened virtual hits. The QED and QED_w values range from 0.38 to 0.84 and 0.37 to 0.80, respectively. The compounds having QED value above 0.4 were selected for further analysis by molecular docking analysis.

Molecular docking

Molecular docking analysis was performed at the active site of PDE4B and PDE4D to reduce the false-positive hits from virtual screening and to identify features essential for the selective inhibition of PDE4B. The docking protocol was validated by re-docking the co-crystallized ligand, rolipram, in the active site of PDE4B (PDB ID: 1RO6) and PDE4D (PDB ID: 1TBB) with an RMSD of 0.328Å and 0.356Å, respectively. The phenyl group of rolipram was sandwiched between the side-chains of Phe446 and Ile410, methoxy group has occupied the small

pocket made up of Tyr403, Tyr233, Thr407, Pro396, Gln443, Asn395, Ile410 and Trp406. The oxygen atom has shown the hydrogen bond interaction with the side-chain NH2 of Gln443. Phenyl ring has shown the π-π interaction with Phe446.

Along with the screened virtual hits, five most selective PDE4B and five most selective PDE4D inhibitors were docked into the active site of PDE4B and PDE4D. **Fig. 5** shows the docking score and inhibitory activity of selective PDE4B and PDE4D inhibitors. All the selective PDE4B inhibitors were showing high docking score in comparison to the PDE4D inhibitors and vice-versa. The most selective PDE4B inhibitor (compound **S6_5**) in the active site of PDE4B and PDE4D is shown in **Fig. 6**. In case of PDE4B, all the selective inhibitors were showing the π-π interaction with Phe446 and the hydrogen bond interaction with Gln443 and His234. The observed binding interaction patterns were complementary with that of pharmacophoric ring aromatic and hydrogen bond acceptor features, which confirm that the developed pharmacophore hypothesis have good predictability. Furthermore, most selective PDE4B inhibitors have shown charge interaction with magnesium metal ion. The residue Met347 controls the access of inhibitors to magnesium metal ion. Whereas, in case of PDE4D, selective inhibitors were unable to form the charge interaction with the magnesium ion and the hydrogen bond interaction with His234 due to movement of Met273 side chain.

Hits showing difference of greater than 1.5 in the docking score were selected and analyzed for the binding mode. Finally, top ten hits (**Fig. 7**) were selected based on Hypo1_estimated IC_{50}, docking score, binding mode, FitValue, and QED value. Molecular superimposition of these hits with the most active and selective compound of the training set revealed that these hits show similar binding orientation in the active site. Further, search by PubChem [33] and SciFinder [34] scholar search tools confirmed that these compounds were not reported as PDE4 inhibitors. Hence, we suggest that these ten compounds could be novel as PDE4B inhibitors.

Biological evaluation

The hits obtained from pharmacophore based virtual screening and molecular docking analysis were purchased from respective vendors and initially evaluated for PDE4B inhibitory activity using the PDE4B2 Assay Kit from BPS BioScience. Rolipram was used as standard during the assay. **Table 4** lists the PDE4B inhibitory activity (nM) for ten virtual hits, indicating that seven compounds (3, 5, 6, 7, 8, 9 and 10) showed higher PDE4B inhibitory activity (2-461nM) in comparison to the rolipram. Further, to know the selectivity of identified hits toward the PDE4B, these hits were evaluated for PDE4D inhibitory activity using the PDE4D2 Assay Kit from

BPS BioScience. Out of ten, six compounds (3, 5, 6, 7, 8 and 10) have shown potent and selective PDE4B inhibitory activity.

Conclusions

We developed ligand-based pharmacophore models for a diverse class of PDE4B and PDE4D inhibitors. The best pharmacophore hypotheses Hypo1_PDE4B and Hypo1_PDE4D were validated using different methods to evaluate its predictive power over the diverse test set compounds. The highly predictive hypotheses were further used in virtual screening for identification of selective PDE4B inhibitors. Three diverse chemical databases were used in virtual screening. The hits from the virtual screening were filtered based on the estimated activity, FitValue, QED value and molecular docking analysis. The activity of the hit compounds has not been reported in the literature as we explored by PubChem and SciFinder Scholar search tools. Molecular docking analysis reveals that residue Met347 plays an important role in accessing the metal binding pocket. Combining all these results, six new compounds with diverse scaffolds were identified as possible lead candidates for designing of potent and selective PDE4B inhibitors.

Acknowledgement

Rahul P. Gangwal is grateful to Council of Scientific & Industrial Research (CSIR), India for providing Senior Research Fellowship.

References

[1] R.A. Pauwels, and K.F. Rabe, Burden and clinical features of chronic obstructive pulmonary disease (COPD). Lancet. 364 (2004) 613-620.

[2] C.J.L. Murray, and A.D. Lopez, Alternative projections of mortality and disability by cause 1990-2020: Global Burden of Disease Study. Lancet. 349 (1997) 1498-1504.

[3] R.A. Pauwels, A.S. Buist, P.M.A. Calverley, C.R. Jenkins, and S.S. Hurd, Global strategy for the diagnosis, management, and prevention of chronic obstructive pulmonary disease NHLBI/WHO Global Initiative for Chronic Obstructive Lung Disease (GOLD) workshop summary. Am. J. Respir. Crit. Care Med. 163 (2001) 1256-1276.

[4] M. Giembycz, Development status of second generation PDE4 inhibitors for asthma and COPD: the story so far. Monaldi Arch. Chest Dis. 57 (2002) 48-64.

[5] B.J. Lipworth, Phosphodiesterase-4 inhibitors for asthma and chronic obstructive pulmonary disease. Lancet. 365 (2005) 167-175.

[6] J.M. O'Donnell, and H.T. Zhang, Antidepressant effects of inhibitors of cAMP phosphodiesterase (PDE4). Trends Pharmacol. Sci. 25 (2004) 158-163.

[7] S.L.C. Jin, and M. Conti, Induction of the cyclic nucleotide phosphodiesterase PDE4B is essential for LPS-activated TNF-α responses. Proc. Natl. Acad. Sci. USA. 99 (2002) 7628-7633.

[8] S.L.C. Jin, L. Lan, M. Zoudilova, and M. Conti, Specific role of phosphodiesterase 4B in lipopolysaccharide-induced signaling in mouse macrophages. J. Immunol. 175 (2005) 1523-1531.

[9] T.J. Torphy, Phosphodiesterase isozymes molecular targets for novel antiasthma agents. Am. J. Respir. Crit. Care Med. 157 (1998) 351-370.

[10] R.D. Design, Subtype selectivity in phosphodiesterase 4 (PDE4): a bottleneck in rational drug design. Curr. Pharm. Des. 14 (2008) 3854-3872.

[11] M.A. Giembycz, Phosphodiesterase 4 inhibitors and the treatment of asthma: where are we now and where do we go from here? Drugs. 59 (2000) 193-212.

[12] M.A. Giembycz, Life after PDE4: overcoming adverse events with dual-specificity phosphodiesterase inhibitors. Curr. Opin. Pharmacol. 5 (2005) 238-244.

[13] S.L.C. Jin, S.L. Ding, and S.C. Lin, Phosphodiesterase 4 and Its Inhibitors in Inflammatory Diseases. Chang Gung Med. J. 35 (2012) 197-210.

[14] K. Naganuma, A. Omura, N. Maekawara, M. Saitoh, N. Ohkawa, T. Kubota, H. Nagumo, T. Kodama, M. Takemura, and Y. Ohtsuka, Discovery of selective PDE4B inhibitors. Bioorg. Med. Chem. Lett. 19 (2009) 3174-3176.

[15] R. Aspiotis, D. Deschênes, D. Dubé, Y. Girard, Z. Huang, F. Laliberté, S. Liu, R. Papp, D.W. Nicholson, and R.N. Young, The discovery and synthesis of highly potent subtype selective phosphodiesterase 4D inhibitors. Bioorg. Med. Chem. Lett. 20 (2010) 5502-5505.

[16] E.F. Kleinman, E. Campbell, L.A. Giordano, V.L. Cohan, T.H. Jenkinson, J.B. Cheng, J.T. Shirley, E.R. Pettipher, E.D. Salter, and T.A. Hibbs, Striking effect of hydroxamic acid substitution on the phosphodiesterase type 4 (PDE4) and TNF alpha inhibitory activity of two series of rolipram analogues: implications for a new active site model of PDE4. J. Med. Chem. 41 (1998) 266-270.

[17] B. Charpiot, J. Brun, I. Donze, R. Naef, M. Stefani, and T. Mueller, Quinazolines: Combined type 3 and 4 phosphodiesterase inhibitors. Bioorg. Med. Chem. Lett. 8 (1998) 2891-2896.

[18] R. Hersperger, K. Bray-French, L. Mazzoni, and T. Müller, Palladium-catalyzed cross-coupling reactions for the synthesis of 6, 8-disubstituted 1, 7-naphthyridines: a novel class of potent and selective phosphodiesterase type 4D inhibitors. J. Med. Chem. 43 (2000) 675-682.

[19] A. Smellie, S.L. Teig, and P. Towbin, Poling: promoting conformational variation. J. Comput. Chem. 16 (1995) 171-187.

[20] U. Singh, R. Gangwal, R. Prajapati, G. Dhoke, and A. Sangamwar, 3D QSAR Pharmacophore based virtual screening and molecular docking studies to identify novel matrix metalloproteinase 12 (MMP-12) inhibitors. Mol. Simul. 39 (2013) 385-396.

[21] H. Li, J. Sutter, and R. Hoffmann. HypoGen: an automated system for generating 3D predictive pharmacophore models. La Jolla, CA, International Univ Line, 2000.

[22] R. Singh, A. Balupuri, and M.E. Sobhia, Development of 3D-pharmacophore model followed by successive virtual screening, molecular docking and ADME studies for the design of potent CCR2 antagonists for inflammation-driven diseases. Mol. Simul. 39 (2013) 49-58.

[23] G.V. Dhoke, R.P. Gangwal, and A.T. Sangamwar, A combined ligand and structure based approach to design potent PPAR-alpha agonists. J. Mol. Struct. 1028 (2012) 22-30.

[24] A. Cereto-Massagué, L. Guasch, C. Valls, M. Mulero, G. Pujadas, and S. Garcia-Vallvé, DecoyFinder: an easy-to-use python GUI application for building target-specific decoy sets. Bioinformatics. 28 (2012) 1661-1662.

[25] R.P. Gangwal, N.R. Das, K. Thanki, M.V. Damre, G.V. Dhoke, S.S. Sharma, S. Jain, and A.T. Sangamwar, Identification of p38α MAP kinase inhibitors by pharmacophore based virtual screening. J. Mol. Graph. Model. 49 (2014) 18-24.

[26] R. Brenk, A. Schipani, D. James, A. Krasowski, I.H. Gilbert, J. Frearson, and P.G. Wyatt, Lessons learnt from assembling screening libraries for drug discovery for neglected diseases. ChemMedChem. 3 (2007) 435-444.

[27] G.R. Bickerton, G.V. Paolini, J. Besnard, S. Muresan, and A.L. Hopkins, Quantifying the chemical beauty of drugs. Nat. Chem. 4 (2012) 90-98.

[28] A. Bhadauriya, G. Dhoke, R. Gangwal, M. Damre, and A. Sangamwar, Identification of dual Acetyl-CoA carboxylases 1 and 2 inhibitors by pharmacophore based virtual screening and molecular docking approach. Mol. Divers. 17 (2013) 139-149.

[29] Glide 5.5, Schrödinger, LLC, 120 West 45th Street, New York, NY 10036, 2009.

[30] R.X. Xu, W.J. Rocque, M.H. Lambert, D.E. Vanderwall, M.A. Luther, and R.T. Nolte, Crystal structures of the catalytic domain of phosphodiesterase 4B complexed with AMP, 8-Br-AMP, and rolipram. J. Mol. Biol. 337 (2004) 355-365.

[31] K.Y.J. Zhang, G.L. Card, Y. Suzuki, D.R. Artis, D. Fong, S. Gillette, D. Hsieh, J. Neiman, B.L. West, and C. Zhang, A glutamine switch mechanism for nucleotide selectivity by phosphodiesterases. Mol. Cell. 15 (2004) 279-286.

[32] Ambure P.S., Gangwal R.P., and Sangamwar A.T., 3D-QSAR and molecular docking analysis of biphenyl amide derivatives as p38α mitogen activated protein kinase inhibitors. Mol. Divers. 16 (2012) 377-388.

[33] Y. Wang, E. Bolton, S. Dracheva, K. Karapetyan, B.A. Shoemaker, T.O. Suzek, J. Wang, J. Xiao, J. Zhang, and S.H. Bryant, An overview of the PubChem BioAssay resource. Nucleic Acids Res. 38 (2010) D255-D266.

[34] A.B. Wagner, SciFinder Scholar 2006: an empirical analysis of research topic query processing. J. Chem. Inf. Model. 46 (2006) 767-774.

Table 1 Statistical parameters of top 10 pharmacophore hypotheses of PDE4B inhibitors generated using HypoGen algorithm

Hypo no.	Total cost	Cost difference[a]	RMSD[b]	Correlation	Features[c]
Hypo1	98.265	48.266	0.720	0.956	***1HBA,2R***
Hypo2	102.913	43.618	0.978	0.917	***1HBA,2R***
Hypo3	104.133	42.398	1.052	0.903	***1HBA,2R***
Hypo4	105.050	41.481	1.087	0.896	***1HBA,1HYA,1R***
Hypo5	106.056	40.475	1.127	0.887	***1HBA,1HYA,1R***
Hypo6	107.111	39.42	1.167	0.879	***1HBA,1HYA,1R***
Hypo7	107.439	39.092	1.179	0.876	***1HBA,2R***
Hypo8	107.791	38.74	1.192	0.873	***1HBA,2R***
Hypo9	107.792	38.739	1.192	0.873	***1HBA,2R***
Hypo10	108.986	37.545	1.231	0.864	***1HBA,1HYA,1R***

The null cost, the fixed cost and the configuration cost are 146.531, 91.397 and 12.909 respectively; [a]Cost difference between the null and the total cost; [b]RMSD, root mean square deviation; [c]Abbreviation used for features: HBA, hydrogen bond acceptor; HYA, Hydrophobic aliphatic; R, Ring aromatic.

Table 2 Statistical parameters of top 10 pharmacophore hypotheses of PDE4D inhibitors generated using HypoGen algorithm

Hypo no.	Total cost	Cost difference	RMSD[b]	Correlation	Features[c]
Hypo1	101.136	84.796	0.466	0.988	***1HBA,1HYA,2R***
Hypo2	106.320	79.612	0.879	0.954	***1HBA,1HYA,1HYAr,1R***
Hypo3	110.622	75.31	1.011	0.939	***1HBA,1HYA,2R***
Hypo4	110.223	75.709	1.044	0.935	***1HBA,1HYA,1HYAr,1R***
Hypo5	110.425	75.507	1.014	0.939	***2HBA,2HYAr***
Hypo6	113.328	72.604	1.160	0.920	***2HBA,2HYAr***
Hypo7	114.972	70.96	1.196	0.915	***1HBA,1HYA,2R***
Hypo8	115.216	70.716	1.182	0.917	***2HBA,1HYA,1R***
Hypo9	115.807	70.125	1.252	0.906	***1HBA,1HYA,2R***
Hypo10	115.855	70.077	1.250	0.906	***1HBA,1HYA,2R***

The null cost, the fixed cost and the configuration cost are 185.932, 96.940 and 15.088 respectively; [a]Cost difference between the null and the total cost; [b]RMSD, root mean square deviation; [c]Abbreviation used for features: HBA, hydrogen bond acceptor; HYA, hydrophobic aliphatic; HYAr, hydrophobic aromatic; R, Ring aromatic.

Table 3 The statistical parameters obtained from Decoy test

Sr. No.	Parameter	Hypo1_PDE4B	Hypo1_PDE4D
1	Total compounds in database (D)	518	407
2	Total Number of actives in database (A)	14	11
3	Total hits (H_t)	21	15
4	Active hits (TP)	12	10
5	True negative (TN)	495	391
6	Enrichment factor or enhancement (E)	21.14	24.66
7	False negatives (FN=A - TP)	2	1
8	False positives (FP=H_t - TP)	9	5
9	GH score (goodness of hit list)	0.631	0.718
10	Accuracy = (TP+TN)/(TP+TN+FP+FN)	0.978	0.985
11	Precision = TP/(TP+FP)	0.571	0.666
12	Sensitivity = TP/(TP+FN)	0.857	0.909
13	Specificity = TN/(TN+ FP)	0.982	0.987

Table 4 The PDE4B and PDE4D inhibitory activity of top ten virtual hits

Sr. No.	Compounds	PDE4B IC_{50} Value (nM)	PDE4D IC_{50} Value (nM)
1	ZINC05612594	813	672
2	ZINC03008558	2202	1253
3	ZINC01210083	378	3056
4	ZINC27499887	790	>10000
5	ZINC15880786	140	1792
6	ZINC15880845	216	1136
7	ZINC01212527	174	2440
8	ZINC33106106	2	2116
9	ZINC09827866	461	136
10	ZINC03008557	140	209
11	Rolipram	466	180

Figure Captions

Fig. 1 a Chemical features of best PDE4B pharmacophore hypothesis (Hypo1_PDE4B) with their inter-feature distance constraints in angstrom (Å). **b** Chemical features of best PDE4D pharmacophore hypothesis (Hypo1_PDE4D) with their inter-feature distance constraints in angstrom (Å). Hydrogen-bond acceptor indicated as green vectored spheres, hydrophobic features indicated as cyan spheres, ring aromatic indicated as orange vectored spheres and exclusion volumes indicated as gray sphere

Fig. 2 a Alignment of most active PDE4B inhibitor with best pharmacophore hypothesis (Hypo1_PDE4B). **b** Alignment of most active PDE4D inhibitor with best pharmacophore hypothesis (Hypo1_PDE4D). **c** Alignment of least active PDE4B inhibitor with best pharmacophore hypothesis (Hypo1_ PDE4B). **d** Alignment of least active PDE4D inhibitor with best pharmacophore hypothesis (Hypo1_ PDE4D)

Fig. 3 a Scatter plot of predicted pIC_{50} values against experimental pIC_{50} values for PDE4B training (blue triangles) and test set (red diamond's) inhibitors. **b** Scatter plot of predicted pIC_{50} values against experimental pIC_{50} values for PDE4D training (blue triangles) and test set (red diamond's) inhibitors

Fig. 4 a The difference in the cost value of hypotheses between the initial spread sheet and 19 random spread sheets generated after CatScramble run (Fischer randomization test) for PDE4B inhibitors. **b** The difference in the cost value of hypotheses between the initial spread sheet and 19 random spread sheets after CatScramble run (Fischer randomization test) for PDE4D inhibitors

Fig. 5 Left side of the graph shows the pIC_{50} values and docking scores of five most selective PDE4B inhibitors and right side of the graph shows the pIC_{50} values and docking scores of five most selective PDE4D inhibitors

Fig. 6 The docked conformation of the most selective PDE4B inhibitor (compound **S6_5**) into the active site of **a** PDE4B (magenta colour) and **b** PDE4D (green colour)

Fig. 7 Chemical structures of top ten hits obtained through sequential virtual screening process

Figure 1

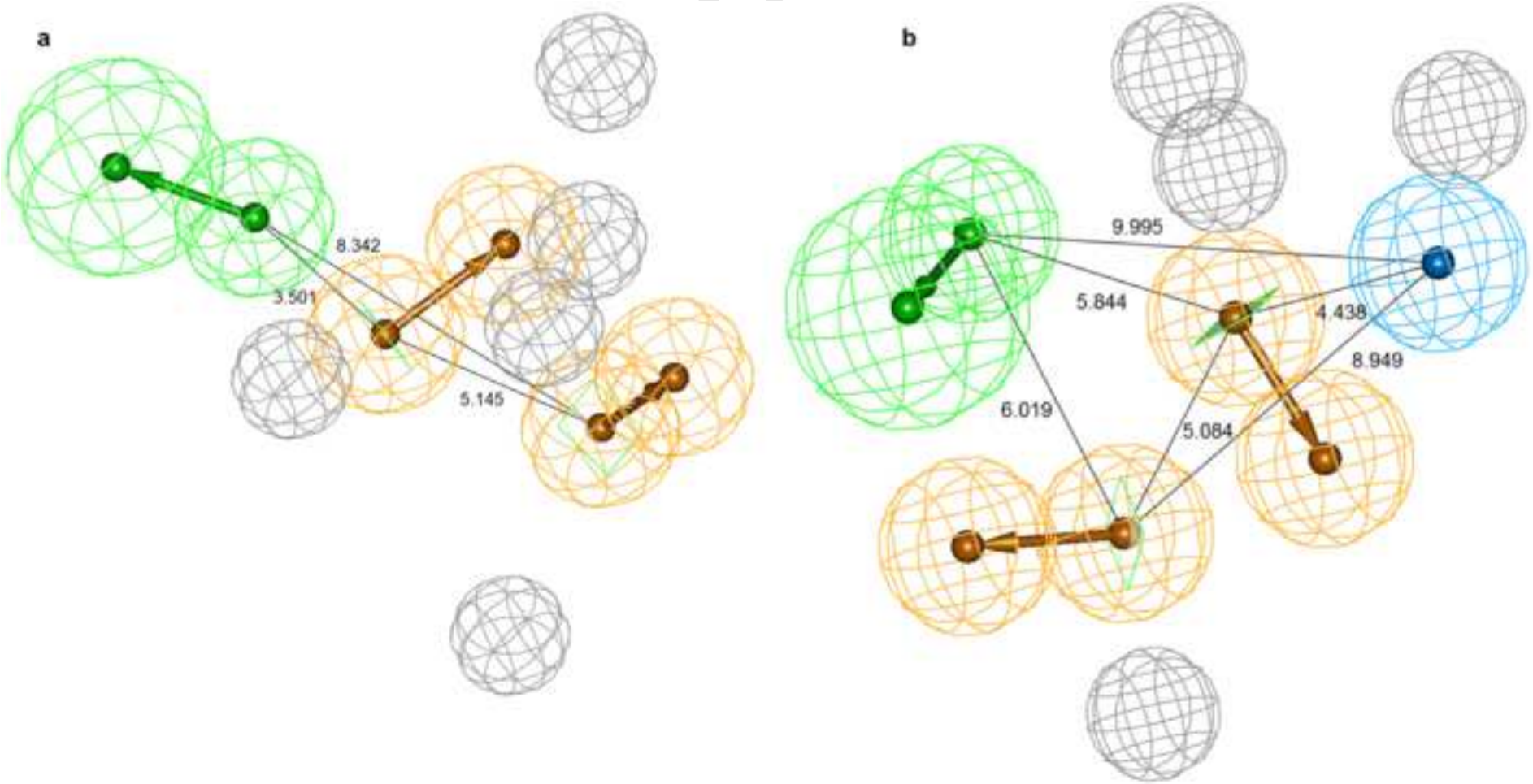

Figure 2

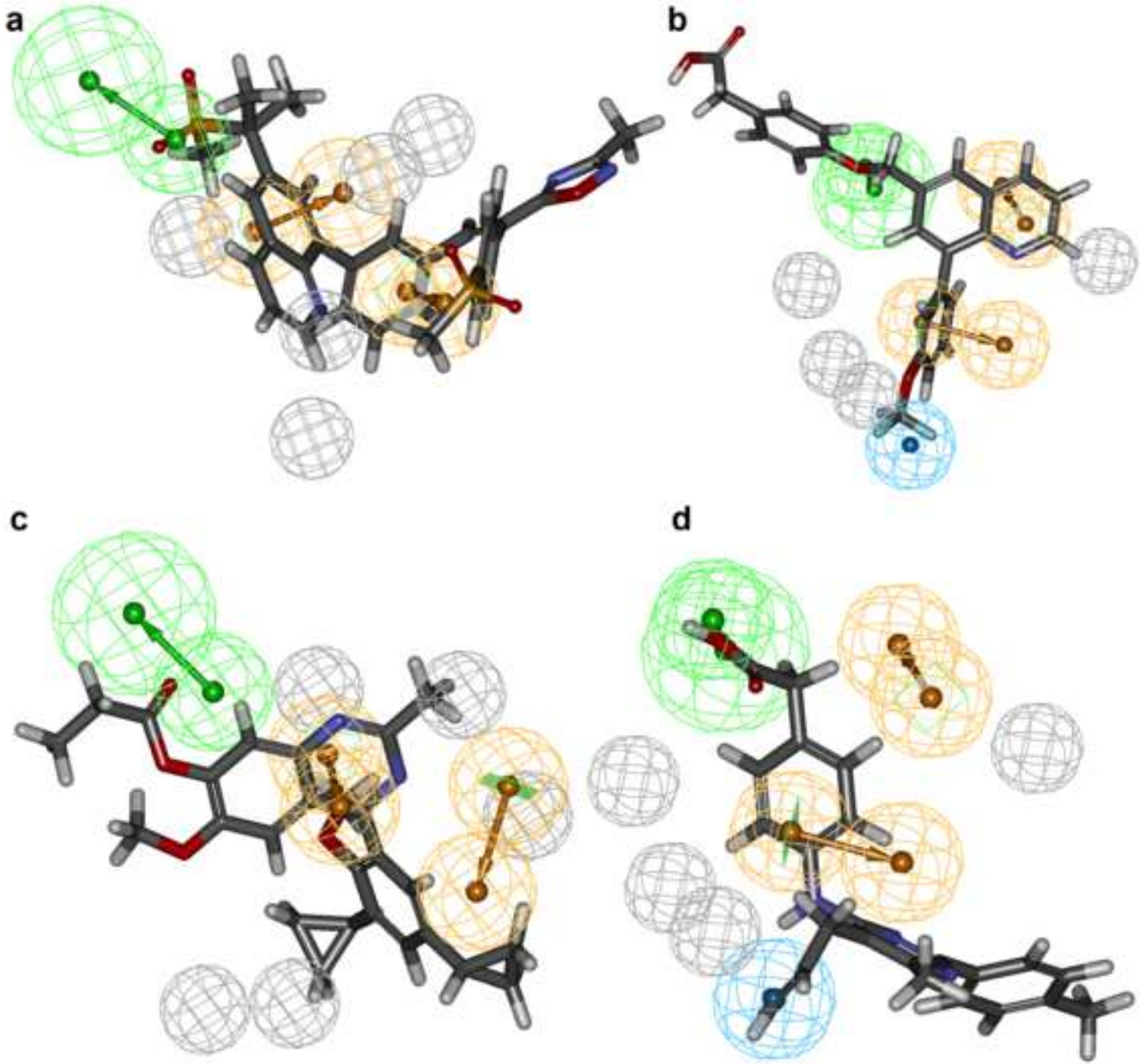

Figure 3

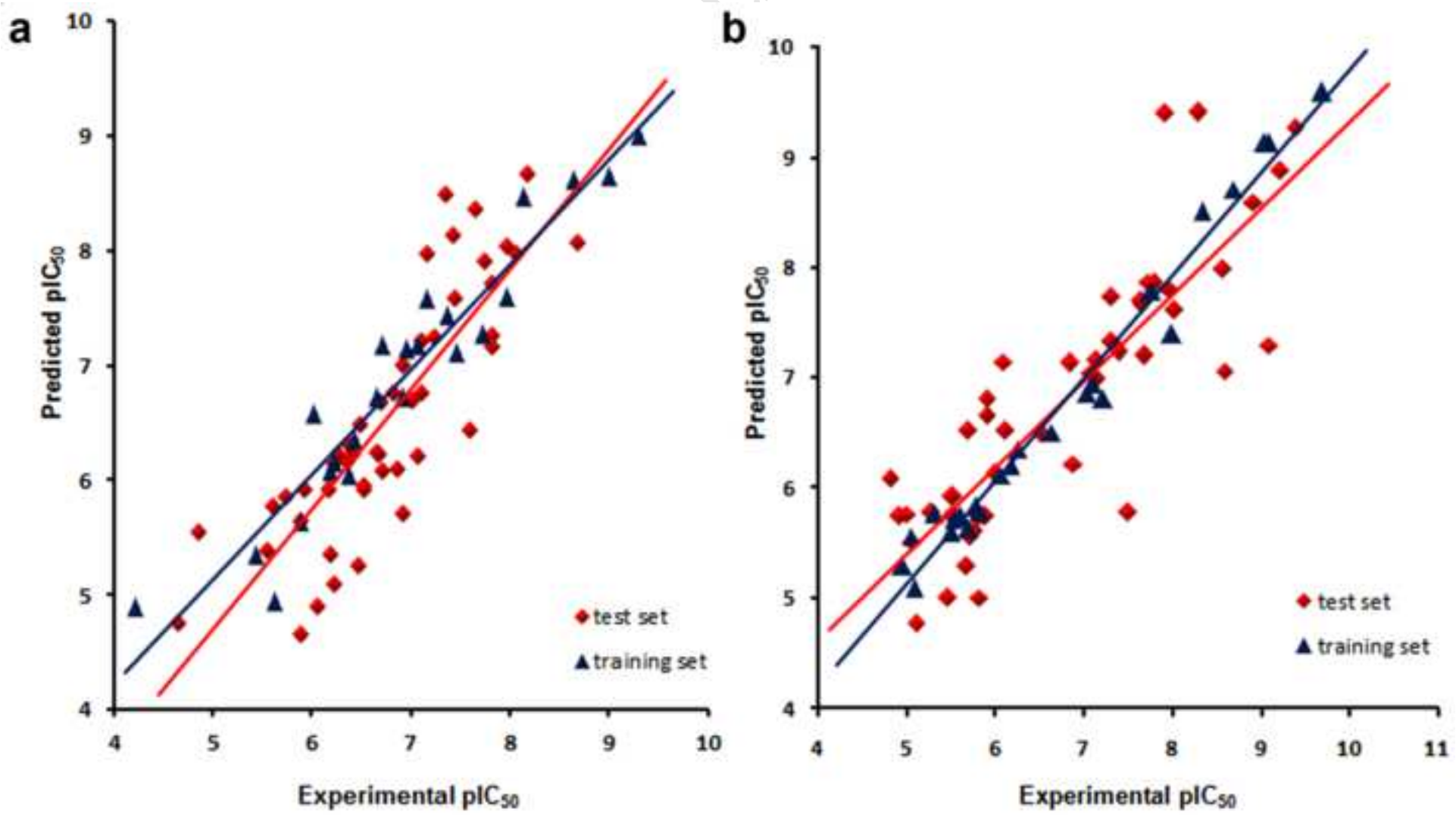
a
Predicted pIC50
Experimental pIC50
test set
training set
b
Predicted pIC50
Experimental pIC50
test set
training set

Figure 4

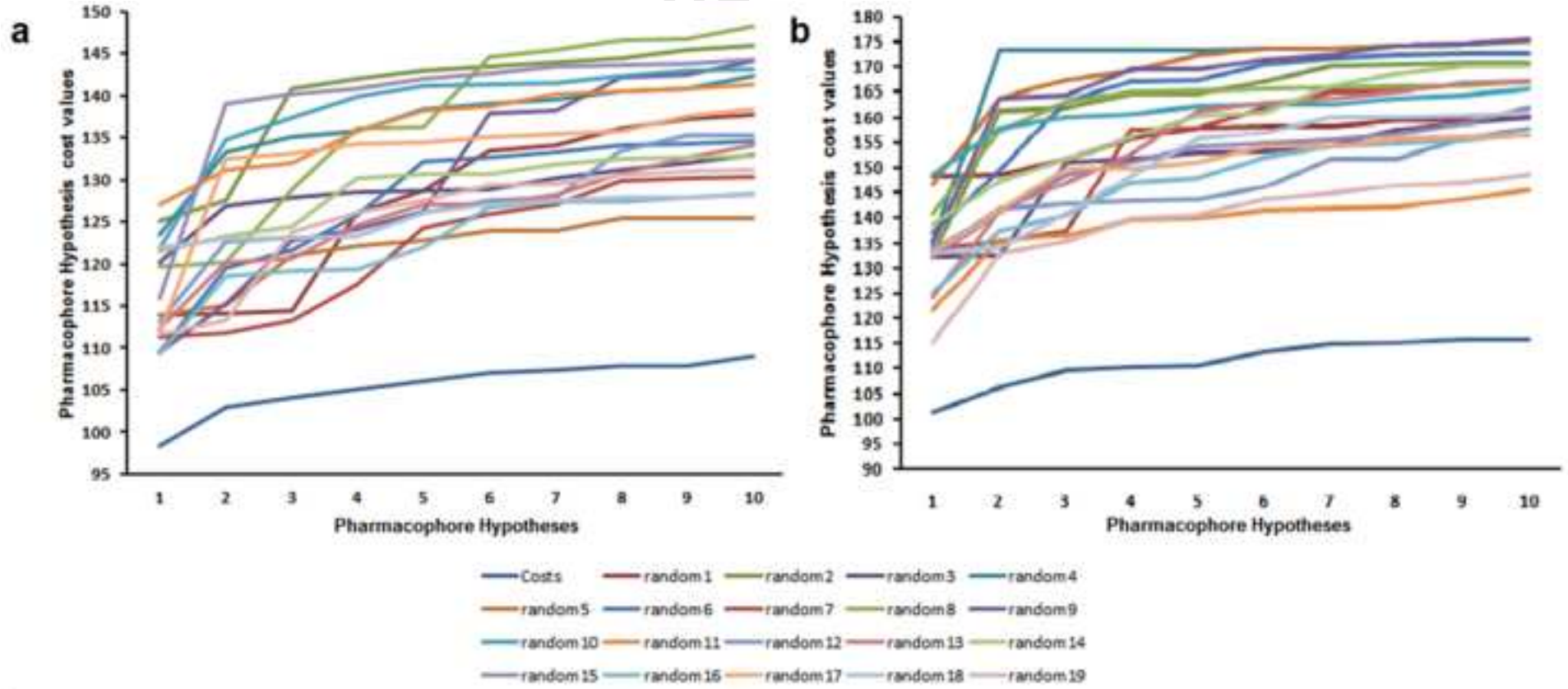
a
Pharmacophore Hypothesis cost values
150
145
140
135
130
125
120
115
110
105
100
95
1 2 3 4 5 6 7 8 9 10
Pharmacophore Hypotheses
b
Pharmacophore Hypothesis cost values
180
175
170
165
160
155
150
145
140
135
130
125
120
115
110
105
100
95
90
1 2 3 4 5 6 7 8 9 10
Pharmacophore Hypotheses
Costs
random 1
random 2
random 3
random 4
random 5
random 6
random 7
random 8
random 9
random 10
random 11
random 12
random 13
random 14
random 15
random 16
random 17
random 18
random 19

Figure 5

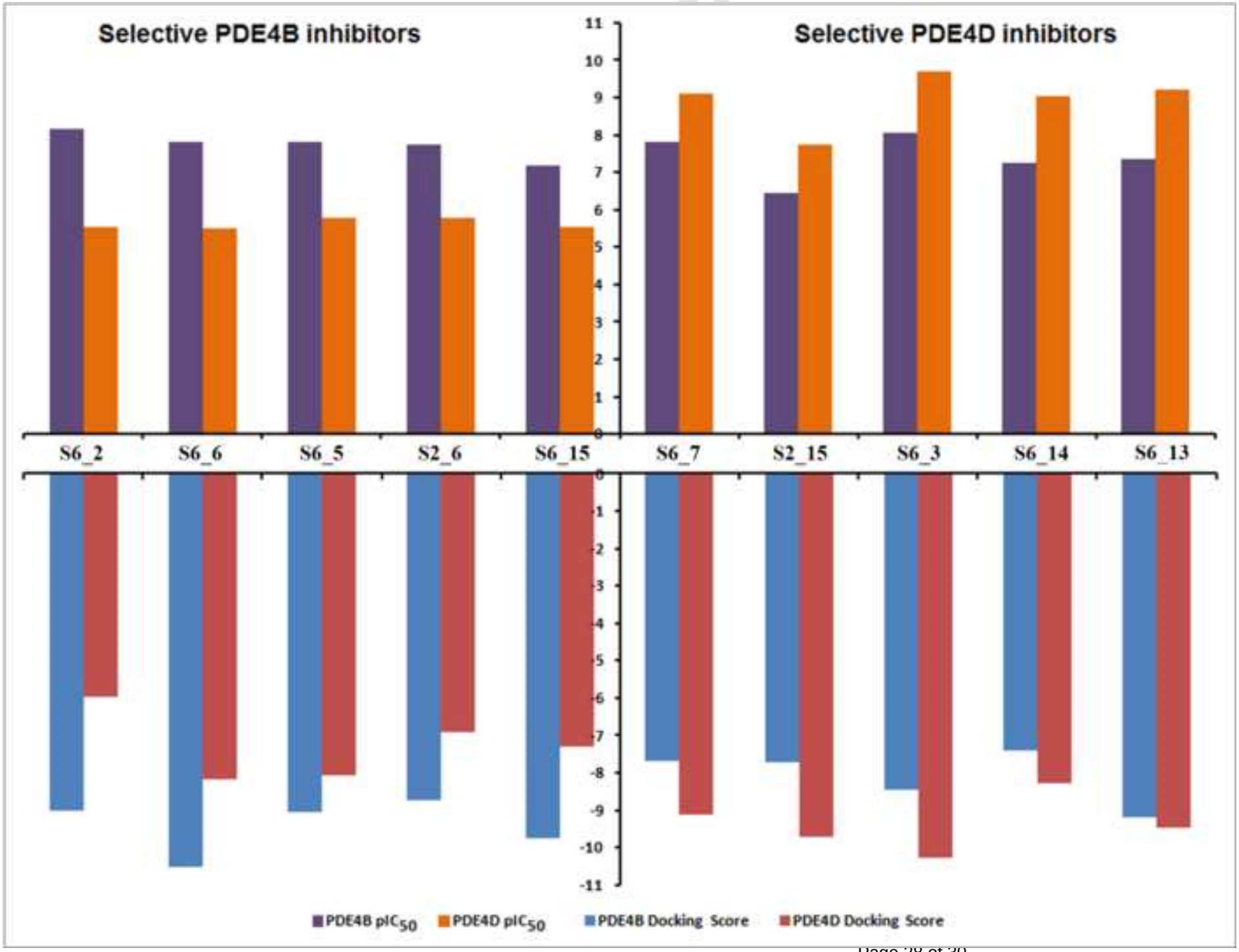
Selective PDE4B inhibitors
Selective PDE4D inhibitors
11
10
9
8
7
6
5
4
3
2
1
0
S6_2
S6_6
S6_5
S2_6
S6_15
S6_7
S2_15
S6_3
S6_14
S6_13
-1
-2
-3
-4
-5
-6
-7
-8
-9
-10
-11
PDE4B pIC50
PDE4D pIC50
PDE4B Docking Score
PDE4D Docking Score

Figure 6

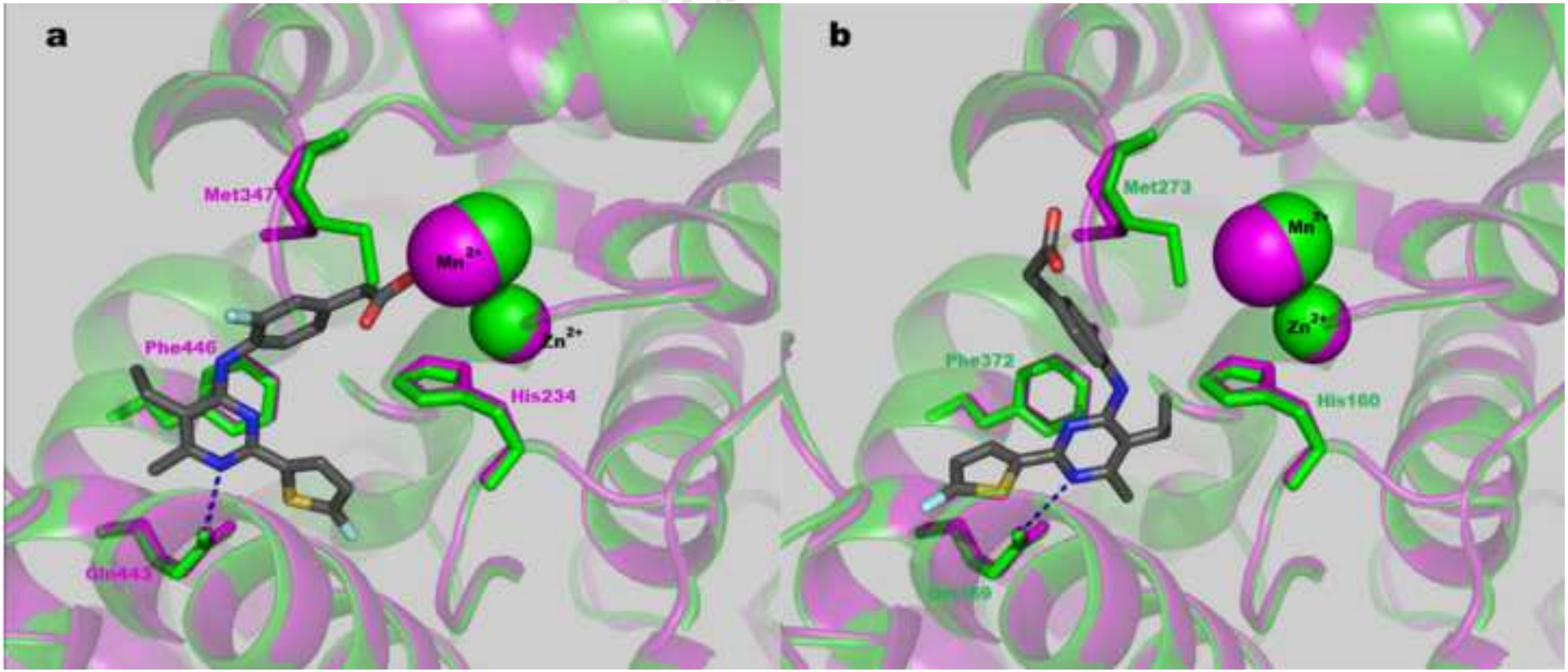
a
Met347
Mn2+
Zn2+
Phe446
His234
Gln443
b
Met273
Mn2+
Zn2+
Phe372
His160

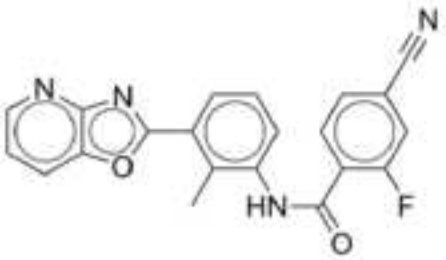

ZINC05612594

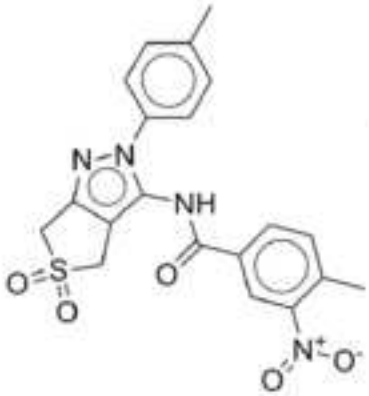

ZINC03008558

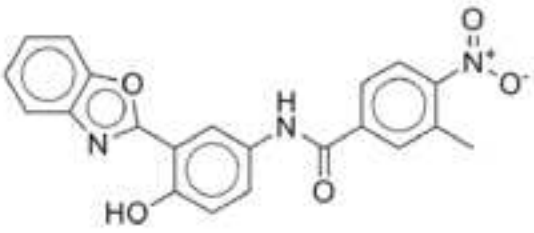

ZINC01210083

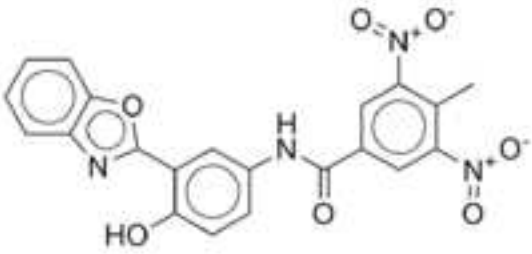

ZINC27499887

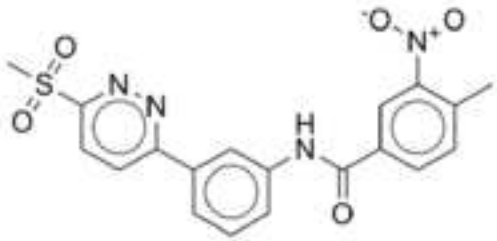

ZINC15880786

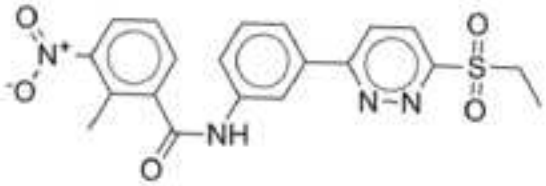

ZINC15880845

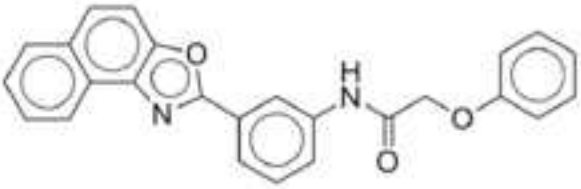

ZINC01212527

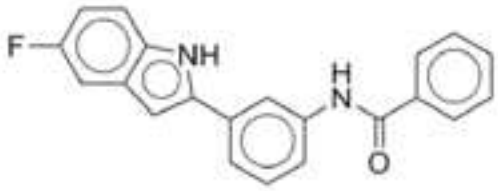

ZINC33106106

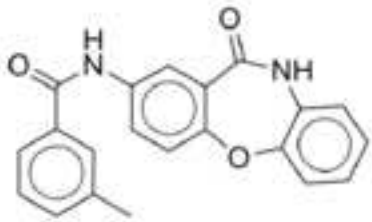

ZINC09827866

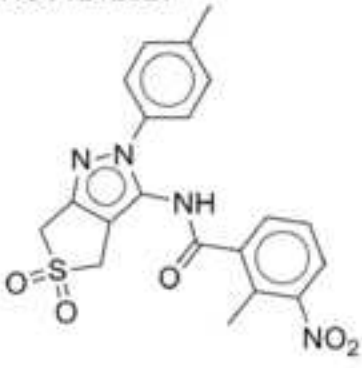

ZINC03008557